CO₂ Detection by Barium Titanate Deposited by Drop Coating and Screen-Printing Methods

Fabien Le Pennec, Amine El Halabi, Sandrine Bernardini, Carine Perrin-Pellegrino, Khalifa Aguir,
and Marc Bendahan

Aix Marseille Univ, Univ Toulon, CNRS, IM2NP, Marseille, France
e-mail: fabien.lepennec@im2np.fr
e-mail: amine.elhalabi@im2np.fr
e-mail: sandrine.bernardini@im2np.fr
e-mail: carine.perrin-pellegrino@im2np.fr
e-mail: khalifa.aguir@im2np.fr
e-mail: marc.bendahan@im2np.fr

Abstract—**Metal Oxide Sensors are promising for gas detection but only a few studies about barium titanium deposition for carbon dioxide detection were reported. Its influence on detection has not been yet fully studied. Herein, we have realised barium titanium sensitive films by drop coating and screen-printing methods. A sensing material solution has been prepared by controlling the viscosity, and then the structural and morphological properties have been studied. The realised sensors were tested in the presence of CO_2 in dry and humid air (20%-50%-70%), in a concentration range from 100 ppm to 5000 ppm. Finally, a cross-interference study has been achieved with SO_2, NO_2 and CO interfering gases.**

Keywords-Gas Sensor; CO₂; BaTiO₃; Metal Oxide; Air Quality.

I. INTRODUCTION

Carbon dioxide (CO_2) is regularly studied as a target gas due to its wide involvement in many circumstances for security, health, or agricultural applications. Our previous work [1] has been focused on CO_2 sensing for the air quality control. CO_2 is present in the air we breathe. Its concentration in outdoor air is around 400 ppm [2]. It is an odorless, colorless, and non-flammable gas. Outdoor CO_2 emissions are mainly of natural origin such as volcanoes, and forest fires, or related to the breathing of animals and plants.

However, a small part of emissions (around a few %) comes from human activities, such as economic development [3], the energy sector (extraction of fossil fuels, electricity production, and heating provided by fossil fuel power plants) [4], agriculture (methane production) [5], industry [6], deforestation [6], transport, or buildings (construction, heating of residential and non-residential buildings) [7], [8]. CO_2 is a molecule also produced by the human body during respiration. Note that our respiratory and circulatory systems are sensitive to the CO_2 concentration. Indeed, an increase in the CO_2 concentration of the inspired air accelerates immediately our breathing rhythm. The CO_2 concentration inside buildings is usually between 350 and 2500 ppm and is related to human occupation and air renewal. Starting at 0.1%, CO_2 becomes a factor in asthma or building syndrome. At 4%, CO_2, the threshold for irreversible health effects is reached and a CO_2 level higher than 10%, can cause death.

The CO_2 measurement can therefore be used as an indicator of air quality [9], [10].

Nowadays, the most commonly used CO_2 sensors are based on infrared phenomena, but this technology is expensive and miniaturization limited. Thus, the challenge of developing a CO_2 gas sensor with a good sensitivity, low-cost, which can provide reliable and reproducible detection results and a fast response to the target gas is increasingly claimed by different companies such as the environment, food industry, and medical. The electrochemical interaction of solid-state gas sensors meets these requirements. Indeed, many materials have been studied, in particular Metal Oxides (MOX) which have promising advantages as mentioned above [11], [12]. Iwata *et al.* [13] and Xiong *et al.* [14] worked on a CO_2 detector based on La_2O_3-SnO_2 and LaOCl-SnO_2, respectively. They obtained a high sensitivity of the sensor to a CO_2 exposure, besides Xiong *et al.* exhibit any saturation to a wide detection range (100 to 20 000 ppm). However, other materials have a high potential for CO_2 detection, such as the barium titanate (BaTiO3) presented in our previous work [1], whose semiconductor behavior is n-type. In 1991, Ishihara *et al.* [15] integrate $BaTiO_3$ in a mixed semiconducting oxide for CO_2 detection by a sensor based on a compressed disk. The combination of CuO-$BaTiO_3$, in equimolar proportion, bring a capacitive response equals to 2.98 for 2% of CO_2. A significant improvement in sensitivity has been achieved by adding silver to the composite. It has increased the sensor response up to 7.74 for 2% of CO_2 [16]. However, the operating temperature was still high (higher than 470°C) and a high concentration (20 000 ppm) was presented, which is not suitable for the air quality control application where the common concentration outdoor is 400 ppm and low energy consumption is required. In addition, M.-S. Lee *et al.* [17] and Keller *et al.* [18] have worked on another approach using a complex mixed semiconducting oxide, $BaTiO_3$-CuO-$LaCl_3$ and $BaTiO_3$-CuO-La_2O_3-$CaCO_3$, respectively. The latter was based on the deposition of a thick film, which was coated by a combination of laser ablation technique and screen printing. The study presents a sensitive layer with a response, R_{gas}/R_{air} = 2.8 for 5000 ppm of CO_2. Moreover, several publications tend to enhance the response to CO_2 through the development of thin films. For example,

TABLE I. SUMMARY OF CO_2 GAS SENSORS BASED ON A COMPOSITE OF $BaTiO_3$ GAS SENSOR

Sensing material	Depositing method	Response definition	Sensitivity	Temp. (°C) / R.H. (%)	Response / Recovery time	Refs.
$BaTiO_3$-CuO-$LaCl_3$	Screen printing	R_g/R_0	2.82 to 10000 ppm	550 / -	-	[17]
$BaTiO_3$-CuO-La_2O_3-$CaCO_3$	Screen printing	R_g/R_0	2.80 to 5000 ppm	600 / -	5 min / -	[18]
CuO-$BaTiO_3$-Ag	RF sputtering	R_g/R_0	1.22 to 5000 ppm	300 / 40	2 min / 3 min	[19]
CuO-$BaTiO_3$-Ag	RF sputtering	R_g/R_0	1.59 to 500 ppm	250 / -	1.5 min / 2 min	[22]
CuO-$BaTiO_3$-Ag	Brush coating	R_g/R_0	1.40 to 700 ppm	120	3 s / 5 s	[23]
$BaTiO_3$	Screen printing	R_g/R_0	1.71 to 400 ppm	280 / 50	2 min / 5 min	This work
$BaTiO_3$	Drop coating	R_g/R_0	1.73 to 400 ppm	280 / 50	2 min / 4 min	This work

Herrán *et al.* [19] carried out a study about $BaTiO_3$-CuO-Ag to improve CO_2 detection. Thus, compared to the use of a thick layer, the radio frequency (RF) sputtering method to obtain a thin metal oxide film brings many benefits, such as the sensitivity or the response/recovery time. However, the main advantage provided by the thin film is its influence on the sensitivity due to the contribution of the metal-semiconductor junction, which has led to a change in resistance [20]. Numerous studies [20, 21, 22] have also shown that it is possible to considerably improve the sensitivity of sensors based on $BaTiO_3$-CuO by the addition of metallic nanograins such as silver. Also, Joshi *et al.* [23] studied this composite and demonstrated a good sensitivity to CO_2 with long-term stability and excellent selectivity for low operating temperature (120°C). In the meantime, few authors report on a study on pure $BaTiO_3$. In Table I, we have presented a literature review of CO_2 sensors based on $BaTiO_3$. The methods of deposition of the sensitive films, the operating temperature, as well as the sensor performances, are summarized. S.B. Rudraswamy *et al.* [24] have shown that $BaTiO_3$ based on a thin film deposited by RF sputtering had a sensitivity to CO_2 equals to R_{gas}/R_{air} = 1.1 for 500 ppm. S. B. Rudraswamy *et al.* and B. Liao *et al.* have shown through their various studies [24], [25] that pure $BaTiO_3$ has no sensitivity to CO_2 in dry air. These observations can be explained by the need for the presence of moisture in the carrier gas mixed with CO_2 to obtain a change in the work function [26]. Therefore, as this material looks promising for CO_2 detection in wet conditions, we decided to manufacture a sensor using $BaTiO_3$ ink to develop sensors that are easy and inexpensive to manufacture.

In this paper, a comparison between the drop coating and the screen-printing methods are presented for the elaboration of $BaTiO_3$ low-cost thick film. The advantages of their use are the speed and the deposition simplicity. Thus, the electrical performances of $BaTiO_3$ during exposure to CO_2 are investigated. Both deposition methods are compared on the basis of several characteristics such as sensitivity,

baseline stability, and response repeatability. The rest of the paper is structured as follows. In Section II, we describe our approach based on $BaTiO_3$ Nano-Powder (NP) deposition on platinum interdigitated electrodes by screen printing and drop coating, low cost, and easily used techniques. Then, in Section III, the detection results are discussed based on a change in the conductance of $BaTiO_3$ during the CO_2 introduction. The detection performances have been studied in a CO_2 concentration range between 100 and 5000 ppm, in the presence of humidity (R.H. 20% 50% and 70%). Finally, a conclusion is given in Section IV.

II. EXPERIMENTAL

This experimental section consists of two parts; in the first part, we have described the sensing film fabrication; in the second part, the measurement system set-up.

A. MOS gas sensors

To carry out our platform test, interdigitated Ti/Pt electrodes, 5 and 100 nm respectively, were deposited by Radio-Frequency (RF) magnetron sputtering on a Si/SiO_2 substrate (Fig. 1).

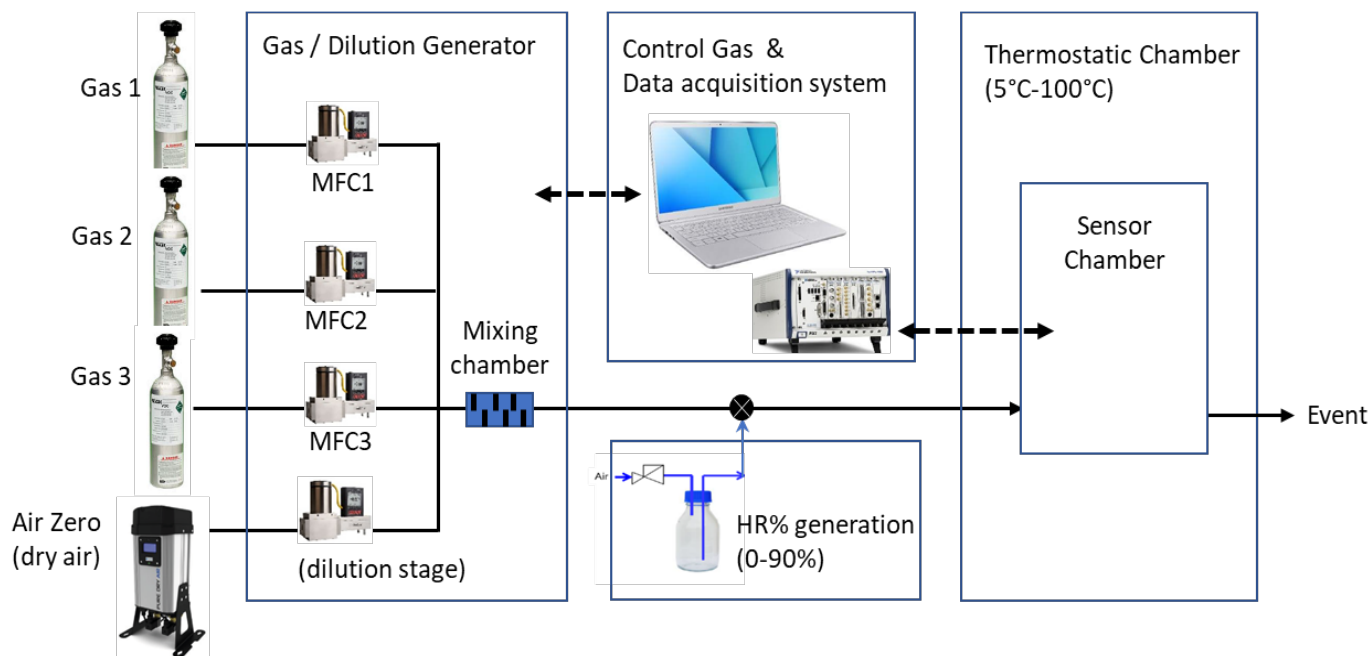Figure 1. Transducer Ti/Pt interdigitated electrodes on a surface of 4x4 mm^2.

Figure 2. Description of the sensor test bench.

0.3g of $BaTiO_3$ Nano Particules (<100 nm, Sigma Aldrich®) was mixed with 0.3g of glycerol for the screen-printing. For the drop coating solution, 0.3g of $BaTiO_3$ NP was diluted in 5 mL of ethanol. Then, the solution was stirred by a magnetic agitator during 2h at room temperature. The solution viscosity has been adjusted to 2.7 mPa.s at 24°C with glycerol measured by the Sine-wave Vibro Viscometer SV-10 instrument. The solution was applied in drops on it using a glass Pasteur pipette. The gas sensors were annealed at 450 °C for 3 min in air ambient to evaporate the organic solvent and ensure the adhesion of the samples to the transducer. Then, the sensitive layer structure and the crystalline phase quality were checked by X-ray Diffraction (XRD) using an Empyrean Panalytical diffractometer equipped with a rapid detector with a theta-theta configuration and CuKα radiation (λ=0.154 nm). The surface investigation was performed by an SEM/EDS acquisition using a ZEISS GeminiSEM 500. Then, the thickness of the deposited $BaTiO_3$ films was measured with a surface profilometry mapping using a Bruker's DektakXT Stylus Profiler.

B. Electrical characterization

The test bench described in Fig. 2, consists of three parts, including a gas and a humidity generation system (0 to 90%), a thermostatically controlled chamber for regulating the temperature during the sensor characterization processes, and a data acquisition system. This equipment allows controlling the dilution of CO_2 in a carrier-neutral gas flow (air). Furthermore, the humidity is generated from the saturation flows of dry air by bubbling it in a container of deionized water, see Fig. 3. The humidity level is then regulated by measuring relative humidity with a capacitive probe and automatically controlling the mixing ratio using two mass flow controllers (MFC4 – MFC5) between the wet flow and the dry flow.
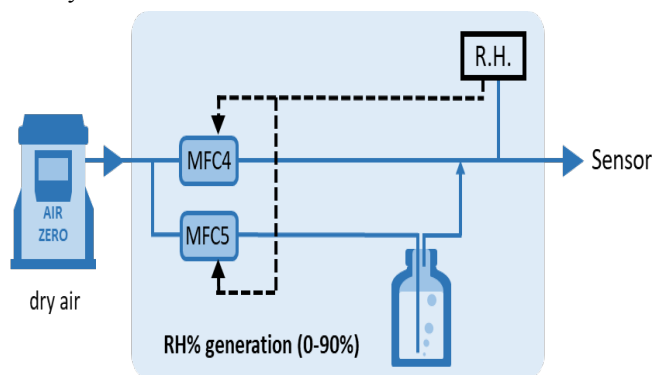

Figure 3. Description of the humidity generation in the air flow.

The gas dilution is precisely controlled by mass flow regulators. The thermostatically controlled chamber allows keeping the test chamber temperature constant during all the processes. The samples were located on a hotplate to control the operating temperature up to 300°C in a thermostatic chamber regulated at 30°C. The electrical measurements and the temperature were monitored by a homemade LabVIEW program to control the Source Measurement Unit (SMU) NI PXie-4141 and the programmable DC power supply NI-PXIe4113, respectively.

For the sensing property investigations, a 1V DC voltage was applied during the current measurements and a constant total flow was maintained by a MFC at 500 Standard Cubic Centimeters per Minute (SCCM). The CO_2 concentrations (from 100 to 5000 ppm) were generated by the mixture of synthetic air and the CO_2 diluted in dry air. Also, the CO_2 exposure was performed during 5 min with three Relative Humidity (RH equals to 20%, 50%, and 70%) to evaluate the sensor response. The sensors were operated at several temperatures from 200°C to 300°C. The best sensor performance compromise for this work was obtained at 280°C. The sensor response is defined in (1):

$$R = R_{gas} / R_{air} \qquad (1)$$

R_{gas} is the sensor resistance under CO_2 exposure and R_{air} is the sensor resistance in the air.

III. RESULTS AND DISCUSSION

In this section, we will present the structural properties of the sensitive layer, and we will discuss our sensor performances.

A. Structural characterization

The XRD pattern presents in Fig. 4a the diffracted X-rays obtained with an Empyrean Panalytical diffractometer (λ=0.154 nm) at room temperature after deposited the screen-printing paste of $BaTiO_3$ on a Si/SiO_2 substrate and annealed it at 450°C during 3 min on a hotplate. Fig. 4b shows the diffracted X-rays obtained in the same conditions for the $BaTiO_3$ layer deposited by drop coating. The both diffractograms present a good agreement with the conventional tetragonal $BaTiO_3$ structure (PDF2 00-05-0626 (ICDD, 2002)) [27]. The $BaTiO_3$ layer deposited by screen printing presents some weak peaks visible in the diffractogram background that are not present in the $BaTiO_3$ layer deposited by drop coating indicating that this method leads to a layer with fewer impurities. For layers deposited by both techniques, the mean grain size was calculated to be 37 ± 2 nm using a single diffraction peak (111) and applying the Scherrer equation given by:

$$\tau = \frac{k * \lambda}{\beta \cos \Theta} \qquad (2)$$

where k = 0.9 and β is the peak FWHM (rad).

The (111) diffraction peak has been chosen as it is a single peak. Therefore, its width is supposed to depend only on grain size and instrumental width. However, the grain size calculation from one peak do not lead to an accurate estimation since it is representative to one preferential orientation.
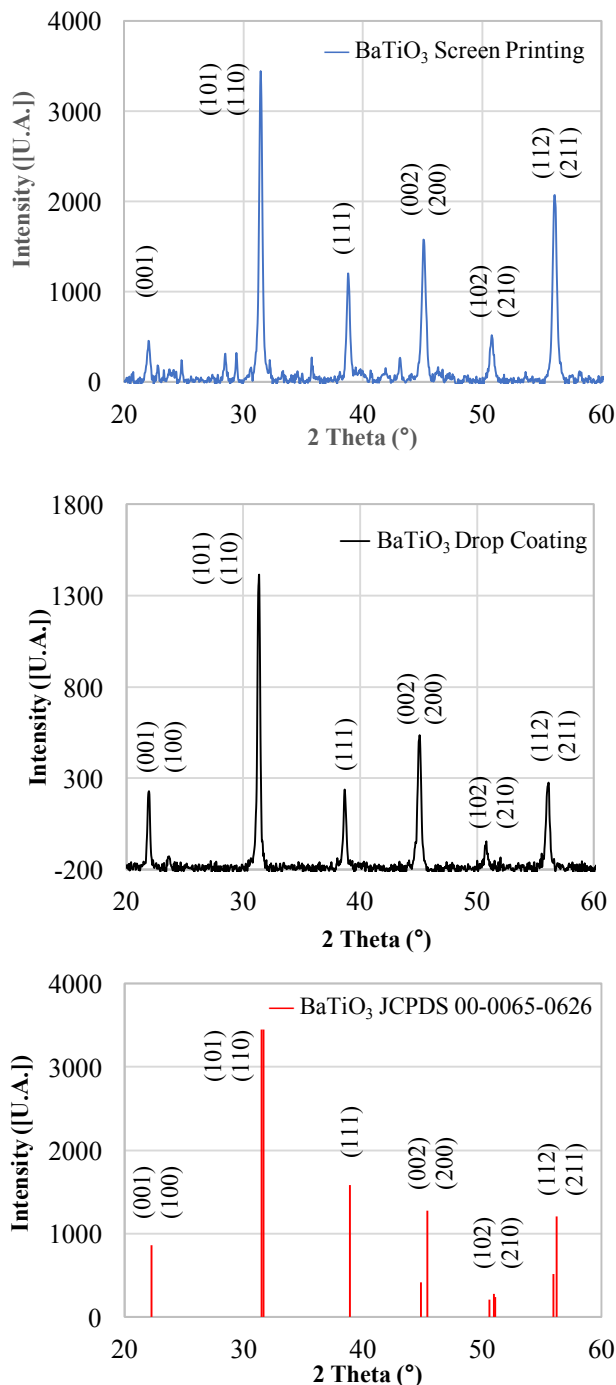

Figure 4. $BaTiO_3$ diffractograms for screen printing sensors (up) and drop coating ones (middle) using $\lambda = 0.154$ nm (Empyrean Panalytical equipment) compared with the reference pattern of the tetragonal structure (down) PDF2 00-05-0626 (ICDD, 2002) [27].

Thus, a scanning electron microscopy (SEM) image produced by a ZEISS GeminiSEM 500 (Fig. 5) enabled us to determine an average grain size which was estimated at 55 nm for both deposition methods.
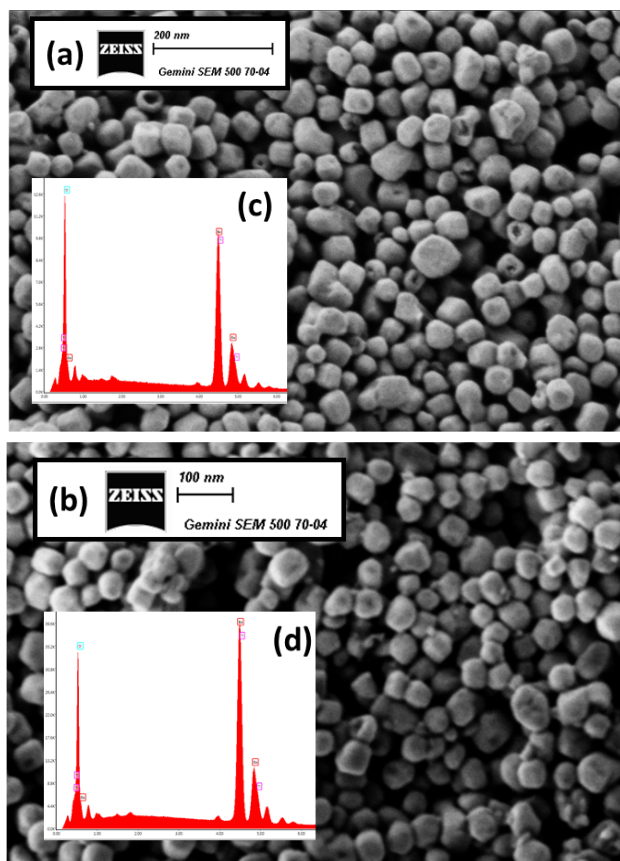

Figure 5. A SEM/EDS analysis have been performed for the both deposit method. SEM images of BaTiO3 (a) screen printing and (b) drop coating. EDS spectra of $BaTiO_3$ (inset) (c) screen printing and (d) drop coating.

The EDS spectra (inset (c) and (d) in Fig. 5) validate the stoichiometry of $BaTiO_3$ listed in Table II. The spectrums of the $BaTiO_3$ reveal the component of Barium (Ba), Titanium (Ti) and Oxygen (O). The EDS analysis is in agreement with the XRD analyses.

TABLE II.   Comparison of Elemental Composition For Screen Printing and Drop Coating Obtained by EDS.

Deposit method	Screen Printing		Drop coating	
Element	Atomic %	Weight %	Atomic %	Weight %
Ba L	24	64.1	21.4	61.3
Ti K	19.7	18.4	18.7	18.7
O K	56.3	17.5	59.9	20.0

The surface morphological images (Fig. 6) were performed by a Bruker's DektakXT Stylus Profiler. The mean thicknesses, are estimated to be 30 µm and 15 µm for the screen printing and drop coating, respectively.
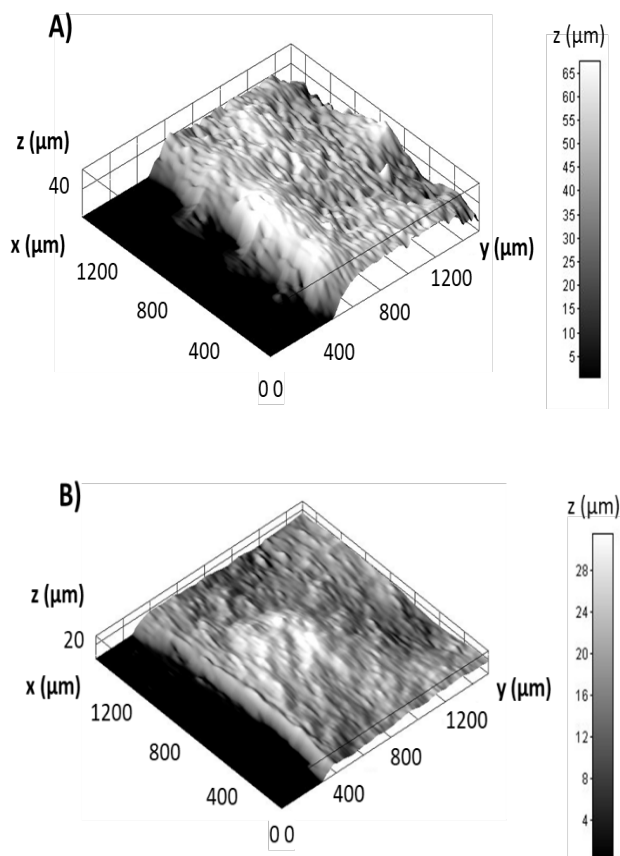

Figure 6. The surface morphological images: A) film surface deposit by screen printing and B) film surface deposit by drop coating.

The surface topography shows a high roughness of our $BaTiO_3$ layer for both deposition methods.

B. Electrical sensor study for screen printing deposition method

Fig. 7 shows a reversible response of the $BaTiO_3$ sensor to 400 ppm of CO_2 gas in 50% RH at 280°C. We observed the sensor resistance increase in the presence of CO_2. Since CO_2 is an oxidant gas, the sensor resistance increase confirms the n-type behaviour of $BaTiO_3$, according to [20]. The response and the recovery times are 2 minutes and 4 minutes, respectively. Where the response time τ_{res} is defined as the time required for the sensor to reach 90% of the sensor response, and the recovery time τ_{rec} as the time needed to reach 10% of the initial resistance baseline after the analyst gas has been purged.
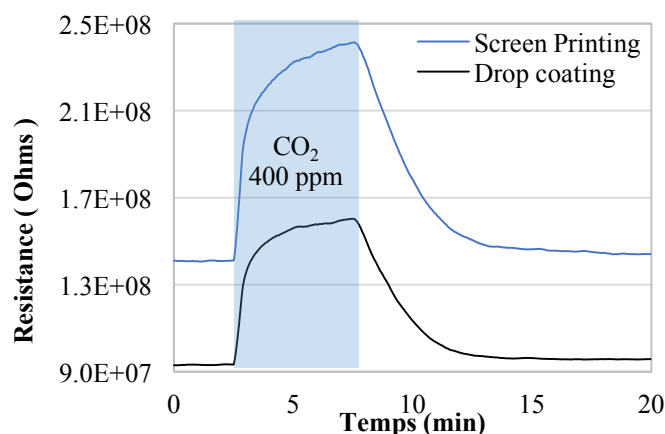
Figure 7. Resistance variation for 400 ppm of CO_2 at 280°C and 50% RH for sensors fabricated by screen printing (up) and drop coating (down).

By maintaining the same operating temperature of 280°C and 50% RH, the CO_2 sensor responses were measured from 100 ppm to 5000 ppm for both sensors and presented in Fig. 8.
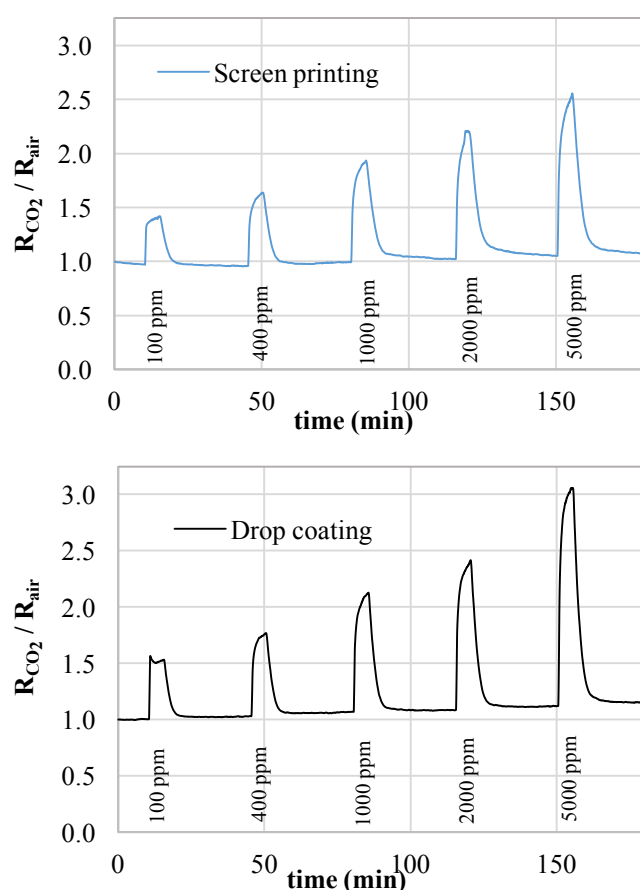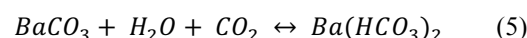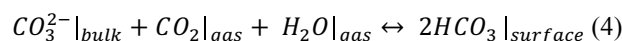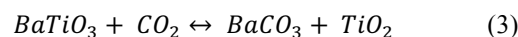

Figure 8. Sensor responses versus CO_2 concentrations (100-5000 ppm, 50% RH at T = 280°C) for screen printing and drop coating $BaTiO_3$ deposition.

In humid conditions and high temperatures, it is assumed that the CO_2 detection phenomenon follows the pathways indicated below [20], [26]:

$$BaTiO_3 + CO_2 \leftrightarrow BaCO_3 + TiO_2 \qquad (3)$$

$$CO_3^{2-}|_{bulk} + CO_2|_{gas} + H_2O|_{gas} \leftrightarrow 2HCO_3|_{surface} \quad (4)$$

$$BaCO_3 + H_2O + CO_2 \leftrightarrow Ba(HCO_3)_2 \qquad (5)$$

The gas sensors provide a measurable response to CO_2 as well as a stable baseline during the experiment. These results showed that our sensors have a wide detection range. It is possible to measure low concentrations with a low signal-to-noise ratio. Table III shows the comparison of the samples regarding their response and recovery times, respectively, tested from 100 to 5000 ppm at 280°C as operating temperature and 50% RH.

TABLE III. COMPARISON OF RESPONSE AND RECOVERY TIMES FOR SCREEN PRINTING AND DROP COATING

Screen printing		
CO_2 (ppm)	response time (min)	recovery time (min)
100	1.7	4.0
400	2.3	5.3
1000	2.8	6.3
2000	2.8	7.4
5000	3.0	6.0

Drop coating		
CO_2 (ppm)	response time (min)	recovery time (min)
100	1.5	4.0
400	2.3	4.2
1000	2.9	4.1
2000	2.4	4.6
5000	2.0	4.5

To study the humidity impact on the sensor responses, three levels of relative humidity (20%, 50 %, and 70%) were introduced into the test chamber and the recorded normalized responses, defined in (1), were evaluated (Fig. 9).
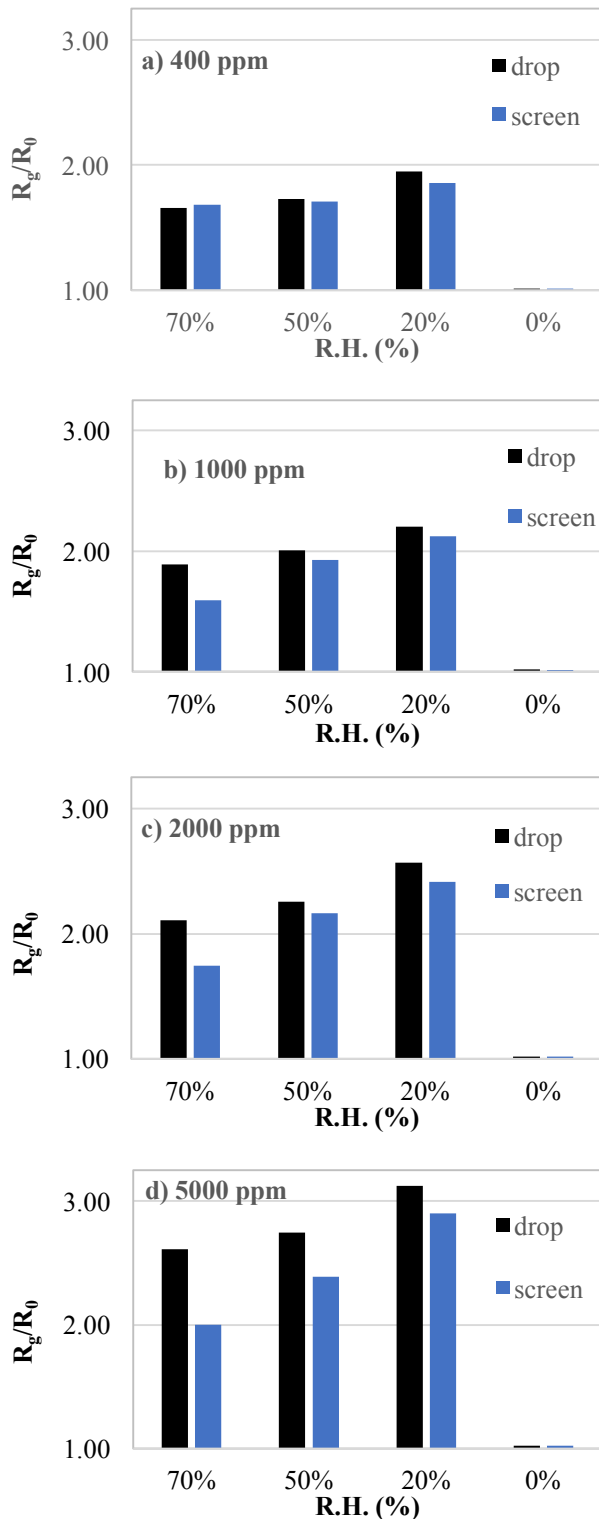
Figure 9. Normalized resistance of BaTiO$_3$ sensor upon CO$_2$ exposure at 280°C and with four relative humidity:
a) 400 ppm, b) 1000 ppm, c) 2000 ppm, d) 5000 ppm.

We have noticed that the humidity has an impact on the CO$_2$ response. For the different concentration levels, the sensor responses increase as humidity decrease. Therefore, optimal sensor responses were determined for 20% humidity. Table IV lists the CO$_2$ response values as a function of humidity and deposition method.

TABLE IV. A SUMMARY OF CO$_2$ RESPONSES BASED ON R$_G$/R$_0$ FROM FIG. 9

Screen printing			
CO$_2$ (ppm)	70%	50%	20%
100	1.50	1.46	1.62
400	1.68	1.71	1.86
1000	-	1.93	2.12
2000	1.74	2.16	2.41
5000	2.00	2.39	2.90

Drop coating			
CO$_2$ (ppm)	70%	50%	20%
100	1.47	1.53	1.64
400	1.66	1.73	1.95
1000	1.89	2.01	2.20
2000	2.11	2.26	2.57
5000	2.61	2.75	3.13

In addition to sensitivity, reproducibility was examined in another set of experiments. However, the repeatability characteristics of the sensors were obtained at 50% RH, which is the value commonly used in the industrial sector. These results are presented in Fig. 10 and show good reproducibility of conventionally prepared sensors. Furthermore, we calculated the coefficient of variation (Table V) to evaluate the repeatability features, defined in (3):

$$C_v = \text{SD} / x_{moy} \qquad (3)$$

where SD is the standard deviation and x$_{moy}$ the average of the normalized response for CO$_2$ exposure.
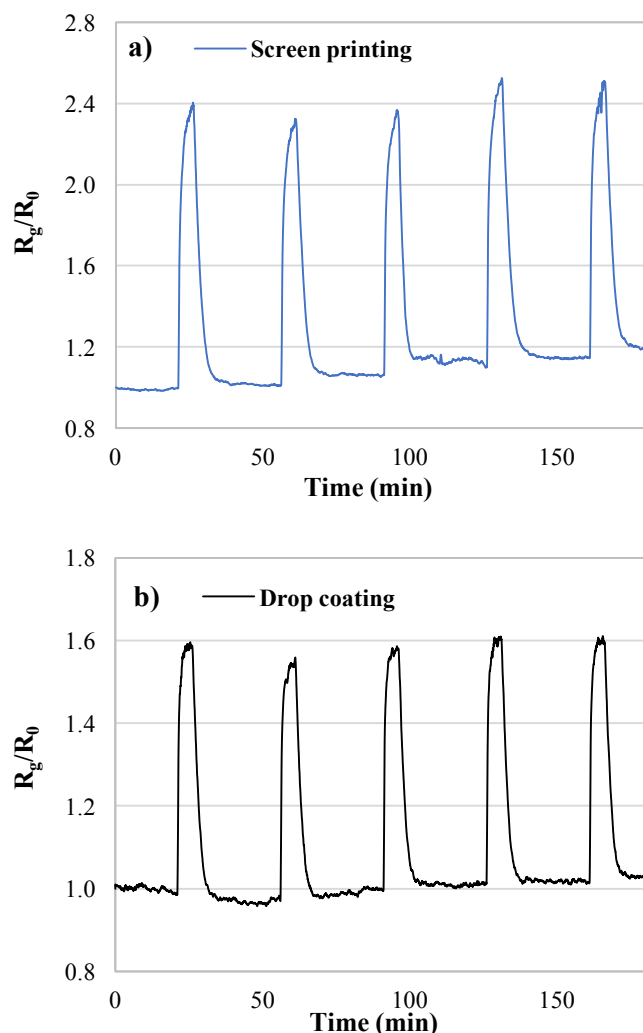
Figure 10. Normalized resistance of BaTiO$_3$ sensors for five exposures of 1500 ppm CO$_2$ at 280°C and 50% RH, a) screen printing and b) drop coating.

We determined a C$_v$ equals to 2.84 % and 1.24 % for the sensors prepared by screen printing and drop coating, respectively. It indicates good repetition behaviour during each CO$_2$ exposure.

TABLE V.   A SUMMARY OF CO$_2$ RESPONSES BASED ON R$_G$/R$_0$ FROM FIG.10

	R$_g$/R$_0$					C$_v$ (%)
Screen printing	2.27	2.20	2.26	2.35	2.42	2.84
Drop coating	1.60	1.62	1.59	1.62	1.64	1.24

As MOX sensors are known for their poor selectivity, a cross sensitivity study of our BaTiO$_3$ sensors to three other greenhouse gases was carried out and is presented in Fig. 11.
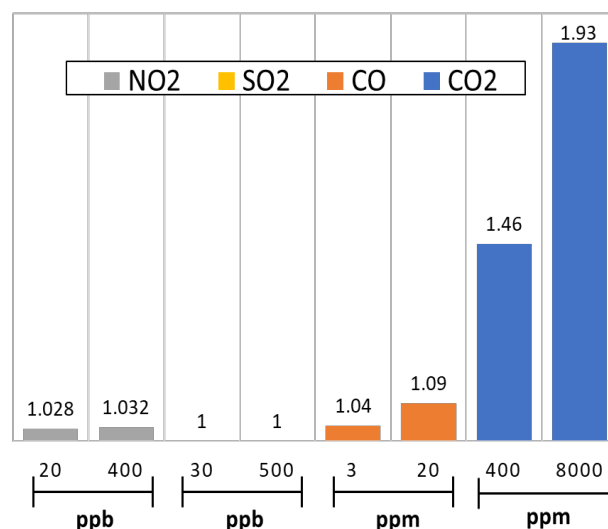

Figure 11. Selectivity study for four gases: NO$_2$, SO$_2$, CO, and CO2. Variation of the normalized resistance of BaTiO$_3$ sensors depending on the gas concentrations.

The gas concentrations chosen are based on the exposure limit value recommended by health agencies. This figure highlighted that our BaTiO$_3$ NP-based sensors have a high sensitivity to CO$_2$ compared to other gases.

IV.   CONCLUSION

Metal Oxide are often studied to find the best materials to fabricate miniaturized and inexpensive sensors. However, the deposition method also influences the properties of the sensors. In this work, two methods of BaTiO$_3$ NP deposition were compared: screen printing and drop coating. The crystalline quality of the deposit was then checked for both sensor series. The sensitive layers formed by the BaTiO$_3$ material were tested as CO$_2$ sensors at an optimized temperature of 280°C and three relative humidity values. The CO$_2$ concentration is proportional to the increasing resistance of the sensitive layer and the sensor baselines are relatively stable during the experiment. Moreover, the sensor response increases with a lower level of humidity in the carried gases. The BaTiO$_3$ sensors have good repeatability feature to CO$_2$ exposure. For the sensors fabricated by screen printing, the response and the recovery times were determined to be 2 min 30 s and 6 min, respectively, and 2 min and 4 min for the sensors with droplet coating layers. This work demonstrates a slight improvement in the performances of CO$_2$ sensor with the drop coating method. This observation would be due to a better control of the homogeneity thickness of the sensitive layer.

REFERENCES

[1] F. Le Pennec, S. Bernardini, M. Hijazi, C. Perrin-Pellegrino,K. Aguir, and M. Bendahan, "Screen Printed $BaTiO_3$ for CO_2 Gas Sensor", ALLSENSORS 2020: The Fifth International Conference on Advances in Sensors, Actuators, Metering and Sensing, Copyright (c) IARIA, pp. 24-25, November 2020. ISBN: 978-1-61208-766-5 7

[2] J. Hansen, M. Sato, P. Kharecha, D. Beerling, V. Masson-Delmotte, M. Pagani, M. Raymo, D. L. Royer, and J. C. Zachos, "Target Atmospheric CO_2: Where Should Humanity Aim? ", The Open Atmospheric Science Journal 2(1), pp. 20, May 2008, doi: 10.2174/1874282300802010217

[3] X.-P. Zhang and X.-M. Cheng, "Energy consumption, carbon emissions, and economic growth in China", Ecol. Econ., vol. 68, n° 10, pp. 2706‑2712, August 2009, doi: 10.1016/j.ecolecon.2009.05.011.

[4] Danish, M. A. Baloch, N. Mahmood, and J. W. Zhang, "Effect of natural resources, renewable energy and economic development on CO_2 emissions in BRICS countries", Sci. Total Environ., vol. 678, pp. 632-638, August 2019, doi: 10.1016/j.scitotenv.2019.05.028.

[5] N. H. A. M. Ridzuan, N. F. Marwan, N. Khalid, M. H. Ali, and M.-L. Tseng, "Effects of agriculture, renewable energy, and economic growth on carbon dioxide emissions: Evidence of the environmental Kuznets curve", Resour. Conserv. Recycl., vol. 160, pp. 104879, September 2020, doi: 10.1016/j.resconrec.2020.104879.

[6] A. Shakoor, F. Ashraf, S. Shakoor, A. Mustafa, A. Rehman, and M. M. Altaf, "Biogeochemical transformation of greenhouse gas emissions from terrestrial to atmospheric environment and potential feedback to climate forcing", Environ. Sci. Pollut. Res., August 2020, doi: 10.1007/s11356-020-10151-1.

[7] D. J. Wales, Julien Grand, V. P. Ting, R. D. Burke, K. J. Edler, C. R. Bowen, S. Mintova, and A. D. Burrows, " Gas sensing using porous materials for automotive applications ", Chem. Soc. Rev., vol. 44, n° 13, p. 4290‑4321, July 2015, doi: 10.1039/C5CS00040H.

[8] L. Pérez-Lombard, J. Ortiz, and C. Pout, "A review on buildings energy consumption information", Energy Build., vol. 40, n° 3, p. 394‑398, January 2008, doi: 10.1016/j.enbuild.2007.03.007.

[9] A. P. Jones, "Indoor air quality and health", Atmos. Environ., vol. 33, 28, pp. 4535-4564, December, 1999. doi: 10.1016/S1352-2310(99)00272-1

[10] B. F. Yu, Z. B. Hu, M. Liu, H. L. Yang, Q. X. Kong, and Y. H. Liu, "Review of research on air-conditioning systems and indoor air quality control for human health", Int. J. Refrig., vol. 32, n°1, pp. 3-20, January 2009, doi: 10.1016/j.ijrefrig.2008.05.004.

[11] D. R. Miller, S. A. Akbar, and P. A. Morris, "Nanoscale metal oxide-based heterojunctions for gas sensing: A review", Sens. Actuators B Chem., vol. 204, pp. 250‑272, December 2014, doi: 10.1016/j.snb.2014.07.074.

[12] J. Zhang, X. Liu, G. Neri, and N. Pinna, "Nanostructured Materials for Room-Temperature Gas Sensors", Adv. Mater., vol. 28, pp. 795‑831, February 2016, doi: 10.1002/adma.201503825.

[13] T. Iwata, K. Matsuda, K. Takahashi, and K.Sawada, "CO_2 Sensing Characteristics of a La_2O_3/SnO_2 Stacked Structure with Micromachined Hotplates", Sensors, vol. 17, n°9, pp. 2156, September 2017, doi: 10.3390/s17092156.

[14] Y. Xiong, Q. Xue, C. Ling, W. Lu, D. Ding, L. Zhu, and X. Li " Effective CO_2 detection based on LaOCl-doped SnO_2 nanofibers: Insight into the role of oxygen in carrier gas", Sens. Actuators B Chem., vol. 241, pp. 725-734, March 2017, doi: 10.1016/j.snb.2016.10.143.

[15] T. Ishihara, "Application of Mixed Oxide Capacitor to the Selective Carbon Dioxide Sensor", J. Electrochem. Soc., vol. 138, n° 1, pp. 173-176, 1991, doi: 10.1149/1.2085530.

[16] T. Ishihara, K. Kometani, Y. Nishi, and Y. Takita, "Improved sensitivity of $CuO-BaTiO_3$ capacitive-type CO_2 sensor by additives", Sens. Actuators B Chem., vol. 28, n°1, pp. 49-54, July 1995, doi: 10.1016/0925-4005(94)01539-T.

[17] M.-S. Lee and J.-U. Meyer, "A new process for fabricating CO_2-sensing layers based on $BaTiO_3$ and additives", Sens. Actuators B Chem., vol. 68, n° 1‑3, pp. 293-299, August 2000, doi: 10.1016/S0925-4005(00)00447-0.

[18] P. Keller, H. Ferkel, K. Zweiacker, J. Naser, J.-U. Meyer, and W. Riehemann, "The application of nanocrystalline $BaTiO_3$-composite films as CO_2-sensing layers", Sens. Actuators B Chem., vol. 57, n°1-3, pp. 39-46, September 1999, doi: 10.1016/S0925-4005(99)00151-3.

[19] J. Herrán, N. Pérez, E. Castaño, A. Prim, E. Pellicer, T. Andreu, F. Peiró, A. Cornet, and J.R. Morante, "On the structural characterization of $BaTiO_3–CuO$ as CO_2 sensing material", Sens. Actuators B Chem., vol. 133, n° 1, pp. 315-320, July 2008, doi: 10.1016/j.snb.2008.02.052.

[20] J. Herrán, G. G. Mandayo, and E. Castaño, "Physical behaviour of $BaTiO_3–CuO$ thin-film under carbon dioxide atmospheres", Sens. Actuators B Chem., vol. 127, n° 2, pp. 370-375, November 2007, doi: 10.1016/j.snb.2007.04.035.

[21] A. M. El-Sayet, F. M. Ismail, and S. M. Yakout, "Electrical Conductivity and Sensitive Characteristics of Ag-Added $BaTiO_3$-CuO Mixed Oxide for CO_2 Gas Sensing", J. Mater. Sci. Technol., vol. 27, n° 1, pp. 35-40, January 2011, doi: 10.1016/S1005-0302(11)60022-4.

[22] S. B. Rudraswamy and N. Bhat, "Optimization of RF Sputtered Ag-Doped $BaTiO_3$-CuO Mixed Oxide Thin Film as Carbon Dioxide Sensor for Environmental Pollution Monitoring Application", IEEE Sens. J., vol. 16, n° 13, pp. 5145-5151, July 2016, doi: 10.1109/JSEN.2016.2567220.

[23] S. Joshi, S. J. Ippolito, S. Periasamy, Y. M. Sabri, and M. V. Sunkara, "Efficient Heterostructures of $Ag@CuO/BaTiO_3$ for Low-Temperature CO_2 Gas Detection: Assessing the Role of Nanointerfaces during Sensing by Operando DRIFTS Technique", ACS Appl. Mater. Interfaces, vol. 9, n° 32, pp. 27014-27026, August 2017, doi: 10.1021/acsami.7b07051.

[24] S. B. Rudraswamy, P. K. Basu, and N. Bhat, "$BaTiO_3$ based Carbon-dioxide gas sensor", in 2012 International Conference on Emerging Electronics, Mumbai, India, December 2012, pp. 1-4, doi: 10.1109/ICEmElec.2012.6636269.

[25] B. Liao, Q. Wei, K. Wang, and Y. Liu, "Study on $CuO–BaTiO_3$ semiconductor CO_2 sensor", Sens. Actuators B Chem., vol. 80, pp. 208-214, December 2001, doi: 10.1016/S0925-4005(01)00892-9.

[26] B. Ostrick, M. Fleischer, H. Meixner, and C.-D. Kohl, "Investigation of the reaction mechanisms in work function type sensors at room temperature by studies of the cross-sensitivity to oxygen and water: the carbonate–carbon dioxide system", Sens. Actuators B Chem., vol. 68, n° 1‑3, pp. 197-202, August 2000, doi: 10.1016/S0925-4005(00)00429-9.

[27] M.-I. Baraton, L. Merhari, P. Keller, K. Zweiacker, and J.-U. Meyer, "Novel Electronic Conductance CO_2 Sensors Based on Nanocrystalline Semiconductors", MRS Proc., vol. 536, pp. 341, 1998, doi: 10.1557/PROC-536-341.